16.3.1 Pitching-Moment Equation and Trim Calculation

For conceptual design studies, sizing the horizontal stabilizer based on similar horizontal tail volume coefficients, as described in Raymer Section 6.5, may be sufficient. Often in conceptual design and always in preliminary design the horizontal stabilizer is sized based on analysis of the configuration.

The horizontal stabilizer is sized based on at least four requirements

1. Static Margin with the c.g. at the rearmost location.
2. Control in pitch with full flaps at landing approach speed with the c.g. at the forwardmost location.
3. Takeoff rotation with the c.g. at the forwardmost location.
4. Maximum travel of the center of gravity.

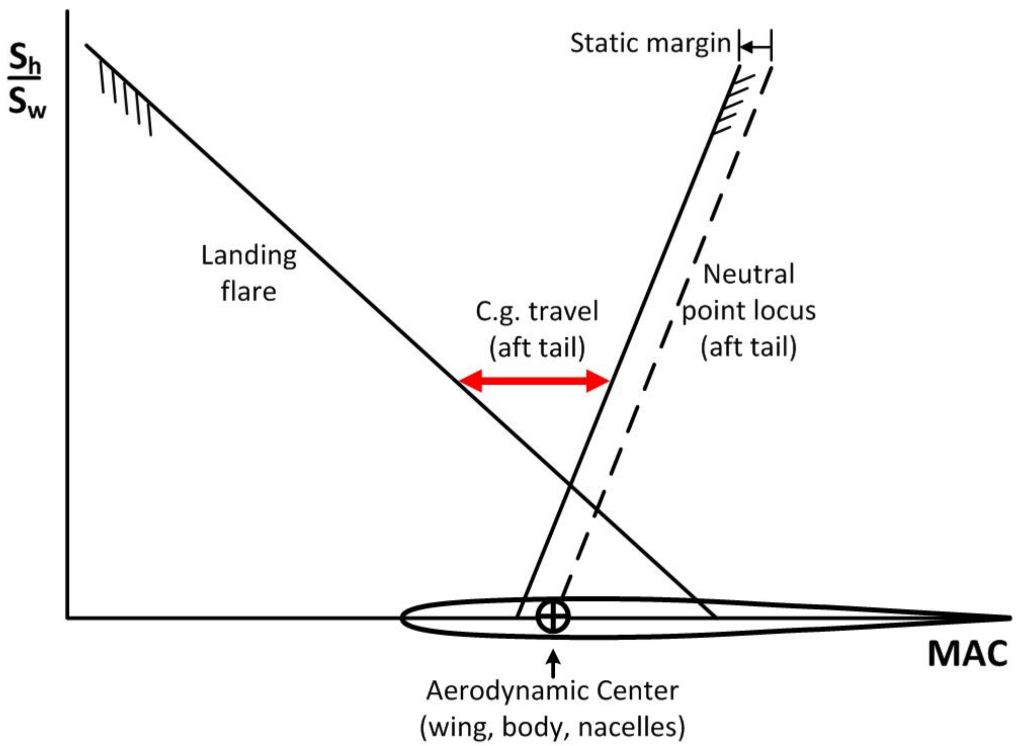

Figure 16.3.1 Notch Chart c.g. Travel Constraints

The chart illustrated above is called a notch chart at Lockheed and a scissors plot at Douglas. This chart is a somewhat simplified version, and does not show the constraint line for takeoff rotation. This constraint is similar to that for landing flare, and it is calculated by determining the pitching moment required to rotate the airplane about the main landing gear just prior to liftoff, with flaps in the takeoff flap setting. The objective is to minimize the horizontal tail area, S_h by matching the fore and aft c.g. travel limits to the stability and control requirements, i.e., by fitting the c.g. travel limits as low as possible into the notch. A typical value of c.g. travel for commercial airplanes is 20% MAC. This matching is done by moving the fuselage forward or aft relative to the wing. Moving the fuselage forward or aft moves the c.g. travel limits forward or aft by a lesser distance, but also affects the stability and control constraint lines. Although somewhat laborious, the analysis can easily be done using a spreadsheet such as the Excel spreadsheet 'Notch' which may be found on the ADAC website under Support > Sample Spreadsheets.

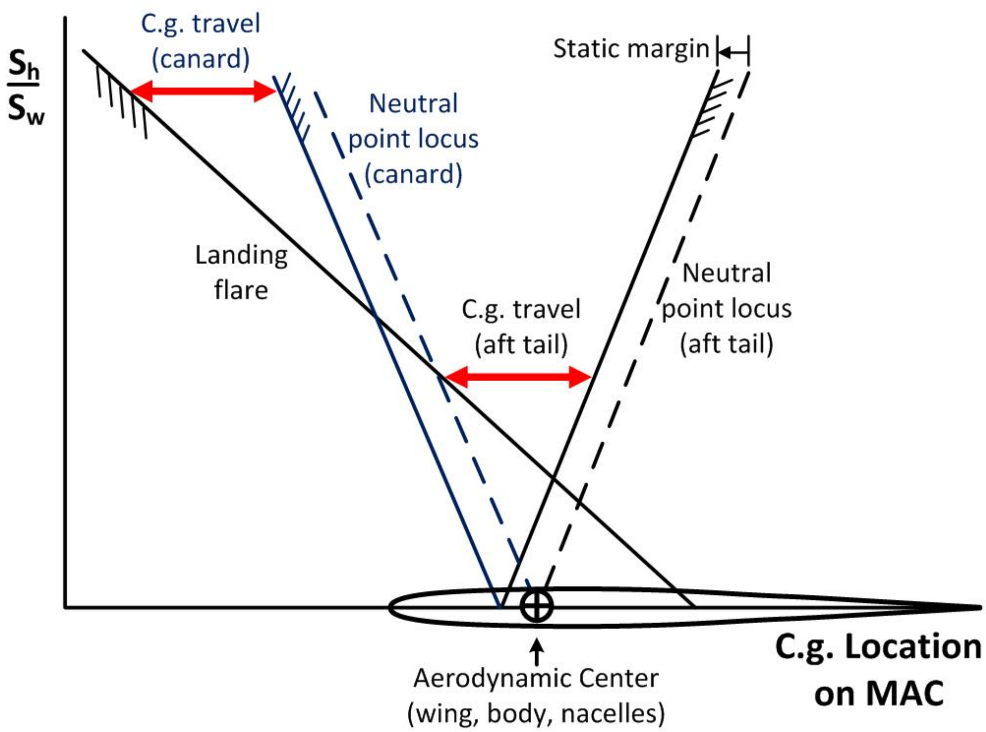

Fig. 16.3.2 Notch Chart c.g. Travel Constraints with Canard

For a canard configuration the terms in Eq. 16.3.5 must be rearranged, and the line representing the change in S_h/S_w with c.g. location rotated forward, as illustrated in Fig. 16.3.2.

The ability to calculate the constraint lines requires that the geometry of the airplane must be reasonably well defined, which is why this determination is usually performed at the preliminary rather than conceptual design stage. The method is described in detail in Torenbeek, Section 9.5.2. Note that the method described in this reference makes allowance for the effect of the change in the weight of the horizontal stabilizer on the center of gravity. This effect is omitted in the spreadsheet referenced above and the description of the procedure described below. Torenbeek also points out that this analysis is somewhat of a simplification of the horizontal stabilizer sizing process, and a complete analysis involves other factors, such as stick forces and dynamic stability.

As Raymer states, the origin is at an arbitrary location, but for these stability and control analyses, the X origin can be conveniently located at the leading edge of the mean aerodynamic chord (LEMAC). The MAC is shown in Fig. 16.3.1.

In this analysis, only the landing approach condition is considered. The procedure for analyzing the takeoff condition is described briefly by Raymer in subsection 16.3.12 Takeoff Rotation on page 625.

As illustrated in Fig. 16.3.1 above, the horizontal stabilizer may be sized by the ability to trim the airplane in landing approach (with full flaps) with forward c.g. condition. This constraint line may be derived from Raymer Eq. (16.7) by expressing $\frac{S_h}{S_w}$ in terms of $\overline{X}_{cg}$ plus the other variables. On landing approach, engine thrust is at idle and can therefore be neglected, as can the inlet sideforce term. The critical condition is at the end of the final approach when in ground effect.

The equation is therefore of the form:

$$\frac{S_h}{S_w} = \frac{C_L\left(\overline{X}_{cg} - \overline{X}_{acw}\right) + C_{m_{w\delta f}}\,\delta_f + C_{m_w} + C_{m_{fus}}}{\eta_h\, C_L\left(\overline{X}_{ach} - \overline{X}_{cg}\right)} \tag{16.3.1}$$

where

C_L = wing lift coefficient, derived from knowledge of wing area, airplane weight, and approach speed

$\overline{X}_{cg}$ = non-dimensional location of the airplane center of gravity, which is a variable in this analysis

$\overline{X}_{acw}$ = non-dimensional location of the wing/body/nacelles aerodynamic center, which is usually at 25% of the MAC

$C_{m_{w\delta f}}$ = wing pitching moment due to flaps, from Eq. (16.20)

δ_f = flap deflection in radians. A maximum of 50^0 for double- or triple-slotted flaps is suggested

C_{m_w} = wing pitching moment, from Eq. (16.19)

$C_{m_{fus}}$ = fuselage pitching moment, derived from Eq. (16.25)

η_h = ratio of dynamic pressure in tail region to free stream dynamic pressure, which (following Raymer's suggestion) can be assumed to be 0.9

C_{L_h} = horizontal stabilizer lift coefficient, from Eq. (16.32)

$\overline{X}_{ach}$ = non-dimensional location of horizontal stabilizer aerodynamic center, which can be assumed to be at 25% of the horizontal stabilizer MAC.

When $S_h/S_w = 0$ then

$$\left(\overline{X}_{cg}-\overline{X}_{acw}\right)=-\frac{C_{m_{w\delta f}}\delta_f+C_{m_w}+C_{m_{fus}}}{C_L} \tag{16.3.2}$$

From Eq. (16.3.2) it can be seen that the X_{cg} value at the intersection of the landing flare constraint with the x-axis is proportional to the pitching moments of the flaps, wing, and fuselage. As the flap angle increases, the line moves to the right.

Unfortunately, derivation of some the terms listed above is not straightforward. The wing pitching moment due to flaps, defined in Eq. (16.20), is

$$C_{m_{w\delta f}}=-\frac{\partial C_L}{\partial \delta_f}\left(\overline{X}_{cp}-\overline{X}_{cg}\right) \tag{16.20}$$

where

$\frac{\partial C_L}{\partial \delta_f}$ = change in wing lift coefficient due to flap deflection, from Eq. (16.17)

$\overline{X}_{cp}$ = non-dimensional location of center of pressure for lift increment due to flaps, which can be derived from Fig. 16.19.

Note that in Fig. 16.19, c' is the MAC of the extended chord of the wing due to Fowler action (e.g., see Fig. 12.17), so the value of x_{cp} calculated from Fig 16.9 must be non-dimensionalized by the MAC, and not by c'.

The change in wing lift coefficient due to flap deflection is given in Eq. (16.17) as

$$\frac{\partial C_L}{\partial \delta_f}=0.9\,K_f\left(\frac{\partial C_l}{\partial \delta_f}\right)_{airfoil}\frac{S_{flapped}}{S_{ref}}\cos\left(\Lambda_{H \cdot L \cdot}\right) \tag{16.17}$$

where

K_f = empirical lift increment correction factor for plain flaps, from Fig. 16.7. For lack of better information, this will have to be used for slotted and Fowler flaps also

$\frac{\partial C_l}{\partial \delta_f}$ = theoretical wing section lift increment for plain flaps, from Fig. 16.6

$\frac{S_{flapped}}{S_{ref}}$ = ratio of wing flapped area to reference area (neglecting flap Fowler action)

$\Lambda_{H \cdot L \cdot}$ = flap hinge line sweep, in radians.

Figure 16.6 applies only to plain flaps, and underestimates the lift increment due to slotted flaps. Torenbeek Fig. 7-24 compares the increase in section lift coefficient for different flap configurations including a plain flap and a double-slotted Fowler flap. From this figure it can be estimated that for double-slotted Fowler flaps, the wing section lift increment from Raymer Fig 16.6 should be factored by 1.7.

The fuselage pitching moment ($C_{m_{fuse}}$) can be derived from Eq. (16.25). If the location of the wing on the fuselage is to be adjusted in order to fit the c.g. travel into the bottom of the notch, the curve may be approximated by

$$K_f = 0.00227\, e^{5.1\left(\frac{L_w}{L_f}\right)} \tag{16.3.3}$$

where

L_w = distance from nose to wing root quarter chord

L_f = fuselage length.

For normal fuselage arrangements, this method will suffice, but for abnormal fuselage shapes, a more detailed method, such as may be found in Ref. 16.3.1. Calculating $C_{m_{fuse}}$ requires multiplying $C_{m_{\alpha fuselage}}$ by α. This can be derived from Eq. (16.13) where α_{OL} is the sum of $\alpha_{OL_{clean}}$ and $\Delta\alpha_{OL_{flapped}}$. The wing incidence on the fuselage (i_w) is a small angle (of the order of 3 degrees).

The horizontal tail lift coefficient is defined in Eq. (16.32)

$$C_{L_h} = C_{L_{\alpha_h}} \left[\left(\alpha + i_w\right)\left(1 - \frac{\partial \varepsilon}{\partial \alpha}\right) + \left(i_h - i_w\right) - \alpha_{OL_h} \right] \tag{16.32}$$

where

$C_{L_{\alpha_h}}$ = horizontal tail lift curve slope, from Eq. (12.6). At the end of the final approach, when in ground effect, his must be increased by about 10%, as indicated by Raymer on page 489

i_h = is the horizontal stabilizer incidence, which on a commercial airplane is set by the trim wheel on the flight deck. A value of -10^0 is suggested for the landing approach condition.

$\frac{\delta \varepsilon}{\delta \alpha}$ = change in downwash due to alpha at horizontal stabilizer, from Fig. 16.12. When in ground effect this term must be reduced by one half, as indicated by Raymer on page 489

The zero-lift angle of attack for the horizontal stabilizer (α_{OL_h}) can be defined as

$$\alpha_{OL_h} = \alpha_{OL_{h\,clean}} + \Delta\alpha_{OL_h} \tag{16.3.4}$$

where

$\alpha_{OL_{h\,clean}}$ = is the angle of attack for zero lift with zero elevator deflection, which is usually zero

$\Delta\alpha_{OL_h}$ = is the change in zero lift alpha for the horizontal stabilizer due to elevator deflection (δ_ε) using Eq. (16.16), and substituting δ_ε for δ_f in Eq. (16.16) and Eq. (16.17). This is the dominant term in the equation. A maximum elevator deflection of -25^0 is suggested.

The dashed line in Fig. 16.3.1 represents the neutral point locus, or the value of $\frac{S_h}{S_w}$ for which an airplane with an aft tail has neutral longitudinal static stability. The critical condition may occur at takeoff, landing approach, or cruise. This value can be calculated by rearranging Raymer Eq. (16.9) into the form:

$$\frac{S_h}{S_w} = \frac{C_{L_\alpha}\left(\overline{X}_{cg} - \overline{X}_{acw}\right) + C_{m_{\alpha fuse}}}{\left(\overline{X}_{ach} - \overline{X}_{cg}\right)\eta_h C_{L_{\alpha_h}} \frac{\partial \alpha_h}{\partial \alpha}} \tag{16.3.5}$$

where

C_{L_α} = gradient of wing lift curve, from Eq. (12.6)

$C_{m_{\alpha fuse}}$ = fuselage pitching moment derivative from Eq. (16.25). Note that the result of Eq. (16.25) is per degree, and therefore must be multiplied by $180/\pi$

$C_{L_{\alpha_h}}$ = gradient of horizontal tail lift curve, from Eq. (12.6)

$\frac{\partial \alpha_h}{\partial \alpha}$ = downwash derivative at tail from Eq. (16.23), using $\frac{\partial \varepsilon}{\partial \alpha}$ from Fig 16.12.

From the information above, the neutral point locus can be constructed. If the airplane is to have a positive static margin (expressed as a percentage of the MAC), a line parallel to the neutral point locus can be drawn that is offset by the static margin. Typical static margin is 5-10% MAC. The foregoing analysis, along with a given allowable c.g. travel, permits Fig. 16.3.1 to be generated.

References

16.3.1 Perkins, C.D., and Hage, R.E., "Airplane Performance, Stability and Control", John Wiley & Sons, 1949.